HELGOLÄNDER MEERESUNTERSUCHUNGEN
Helgoländer Meeresunters. 43, 19–28 (1989)

Spermatogenesis in *Platynereis massiliensis* (Polychaeta: Nereidae)

Joachim Lücht* & Hans-Dieter Pfannenstiel

Institut für Allgemeine Zoologie, Freie Universität Berlin; Königin-Luise-Straße 1–3, D-1000 Berlin 33, Federal Republic of Germany

ABSTRACT: Stage 1 of spermatogenesis in the protandrous polychaete *Platynereis massiliensis* is represented by clusters of about 60 spermatogonia which appear in the coelomic cavity. There are no testes in *P. massiliensis*. The origin of the spermatogonial clusters is not known. Subclusters of approximately 20 primary spermatocytes each represent stage 2. The appearance of synaptonemal figures in the spermatocyte nuclei marks the beginning of stage 3. Cells tend to lose their tight packing during stage 3 but interdigitate with cellular processes. Then very small subclusters of 4 to 8 spermatocytes appear. Meiosis is completed during stage 4, giving rise to secondary spermatocytes and then to spermatid tetrads. Spermatogonia and primary spermatocytes are interconnected by structurally specialized fusomes while secondary spermatocytes and spermatids, which are also in cytoplasmic continuity, show rather simple cell bridges. Synthesis of acrosomal material starts during stage 2. During spermiogenesis the proacrosomal vesicles of Golgi origin travel from the posterior part of the cell to its anterior part to form the acrosome proper. Acrosome formation, nuclear condensation, shaping of the long and slender sperm nucleus, and development of the sperm tail are the main events during spermiogenesis. Sperm morphology is briefly discussed with respect to its phylogenetic bearings.

INTRODUCTION

Production and release of just one batch of gametes per lifetime is a characteristic feature of many nereid polychaetes. This mode of reproduction is called monotely, and it is often accompanied by an epitokous metamorphosis leading to the formation of a so-called heteronereis. *Platynereis dumerilii* shows this mode of reproduction. Interestingly enough, the sibling species *Platynereis massiliensis* is a protandrous hermaphrodite which does not undergo heteronereid modifications (Hauenschild, 1951). In such a case it is beyond any doubt that the strikingly different reproductive modes are of no phylogenetic significance. Consequently, the same should be true for differences observed in spermatogenesis and sperm morphology. At present, there is very little information available on spermatogenesis in *P. dumerilii* and *P. massiliensis* (see Schiedges, 1981; Hofmann et al., 1986; Pfannenstiel et al., 1987). The present paper describes the stages of spermatogenesis and sperm morphology in *P. massiliensis* at the EM level.

Adressee for reprints

MATERIAL AND METHODS

Animals

Our laboratory culture of *Platynereis massiliensis* Moquin-Tandon 1869 originates from adult specimens and eggs and embryos which were collected between 1982 and 1985 in the vicinity of Banyuls-sur-mer (France). Culture requirements are essentially the same as outlined by Hauenschild (1970) for *Platynereis dumerilii* (20° ± 1°C; LD 16:8).

Brooding tubes were opened under a dissecting microscope and the directly developing young worms were transferred to Boveri dishes with 150 ml sea-water. The medium (artificial and natural sea-water 1:1) was changed 2–3 times a week for the next 2–3 months. During that time, the worms were fed spinach and TetraMenü, a commercially available fish food. With approximately 10 setigerous segments (= ss), groups of ca. 120 specimens were transferred to little aquaria (20 × 20 × 6 cm) with 500 ml sea-water. These mass cultures were fed spinach only. Specimens of the desired developmental stages were taken from these aquaria and prepared for EM studies.

Electron microscopy

Specimens were anaesthetized in 6 % $MgCl_2$ in distilled water and fixed in 2.5 % glutaraldehyde in phosphate buffer (pH 7.4, 1050 mOsm) for 1 h at room temperature. After rinsing in the same buffer, specimens were postfixed in 2 % OsO_4 in phosphate buffer (pH 7.4, 1050 mOsm) for 1 h at room temperature. After dehydration through a graded ethanol series (70 % ethanol saturated with uranyl acetate), specimens were passed through propylene oxide and embedded in Araldite. Thin sections (silver-grey) were cut on a Reichert Ultracut with a glass knife, stained with lead citrate, and examined with a Zeiss EM 9-s2 or a Zeiss EM 10 c.

RESULTS

Spermatogenesis

The stages of spermatogenesis are compiled in Table 1. Spermatogonial clusters (stage 1) appear freely floating in the coelomic fluid of approximately 40 day-old specimens with 10–20 ss. Testes are not present, and the origin of these clusters is not known. The spermatogonia of a cluster are interconnected by cytoplasmic bridges. Stage 1 clusters subdivide into smaller units of approximately 20 cells which apparently no longer divide mitotically. These stage 2 subclusters represent primary spermatocytes (Fig. 1). Primary spermatocytes are also in cytoplasmic continuity (Figs 2, 3). Usually, Golgi stacks are found close to fusomes during stage 2. The vesicles of these stacks are proacrosomal vesicles which contribute to acrosome formation (Figs 2, 4, 6). Centrioles are also located in the immediate vicinity of cell bridges (Figs 4, 6). Electron-dense granules and condensations adjacent to bridge membranes (Figs 2, 3) are characteristic features of fusomes. The appearance of synaptonemal complexes (Figs 5, 7) marks the beginning of meiosis. At the same time, the contact between stage 3 cells loosens but the clusters are not yet dispersed. At that stage, cells tend to interdigitate with pseudopodial

Table 1. Stages of spermatogenesis in *Platynereis massiliensis*

Stage	Characteristics
1	Clusters of more than 60 spermatogonia in cytoplasmic continuity enveloped by sheath cells; no subclusters visible;
2	Clusters of primary spermatocytes (approx. 20 cells each) detach from stage 1 clusters; Golgi complexes start to form proacrosomal vesicles;
3	Subclusters of 4 to 8 primary spermatocytes detach from stage 2 clusters and enter meiosis; haploid secondary spermatocytes appear;
4	secondary spermatocytes complete meiosis; spermatid tetrads appear;
5	spermatids undergo spermiogenesis; commonly spermatid tetrads detach from stage 2 clusters prior to spermiogenesis; tetrad flagellae start to beat inside coelomic cavity;

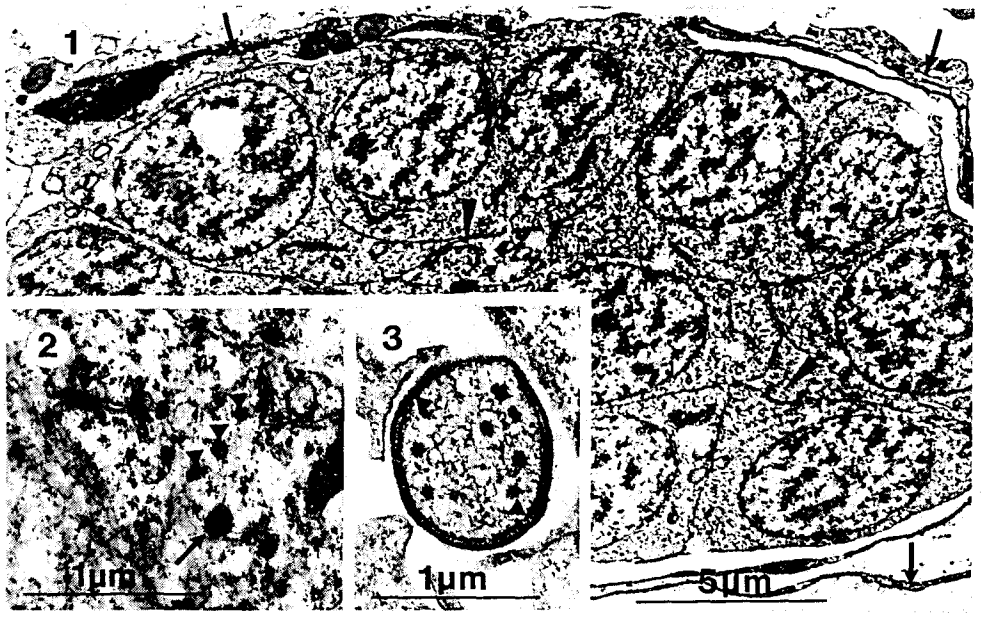

Fig. 1. Electron micrograph (EM) of a stage 2 cluster of primary spermatocytes. Note cell bridges (arrowheads) and eleocytes (arrows) in close contact with spermatocyte cluster

Fig. 2. EM of cell bridge between primary spermatocytes. Note presence of electron-dense granules (arrowheads) which characterize this type of fusome. Arrow – proacrosomal vesicle; double arrowhead – zonula adhaerens

Fig. 3. EM of cell bridge between primary spermatocytes with plane of section perpendicular to that shown in Fig. 2. Note electron-dense material adjacent to bridge membrane (arrowheads)

processes (Fig. 5). Later on, small subclusters of 4 to 8 cells are formed (Fig. 5). During stage 4, meiosis is completed in the cells of the small clusters and each spermatocyte successively gives rise to two secondary spermatocytes (Fig. 8) and then to a spermatid tetrad (Fig. 9).

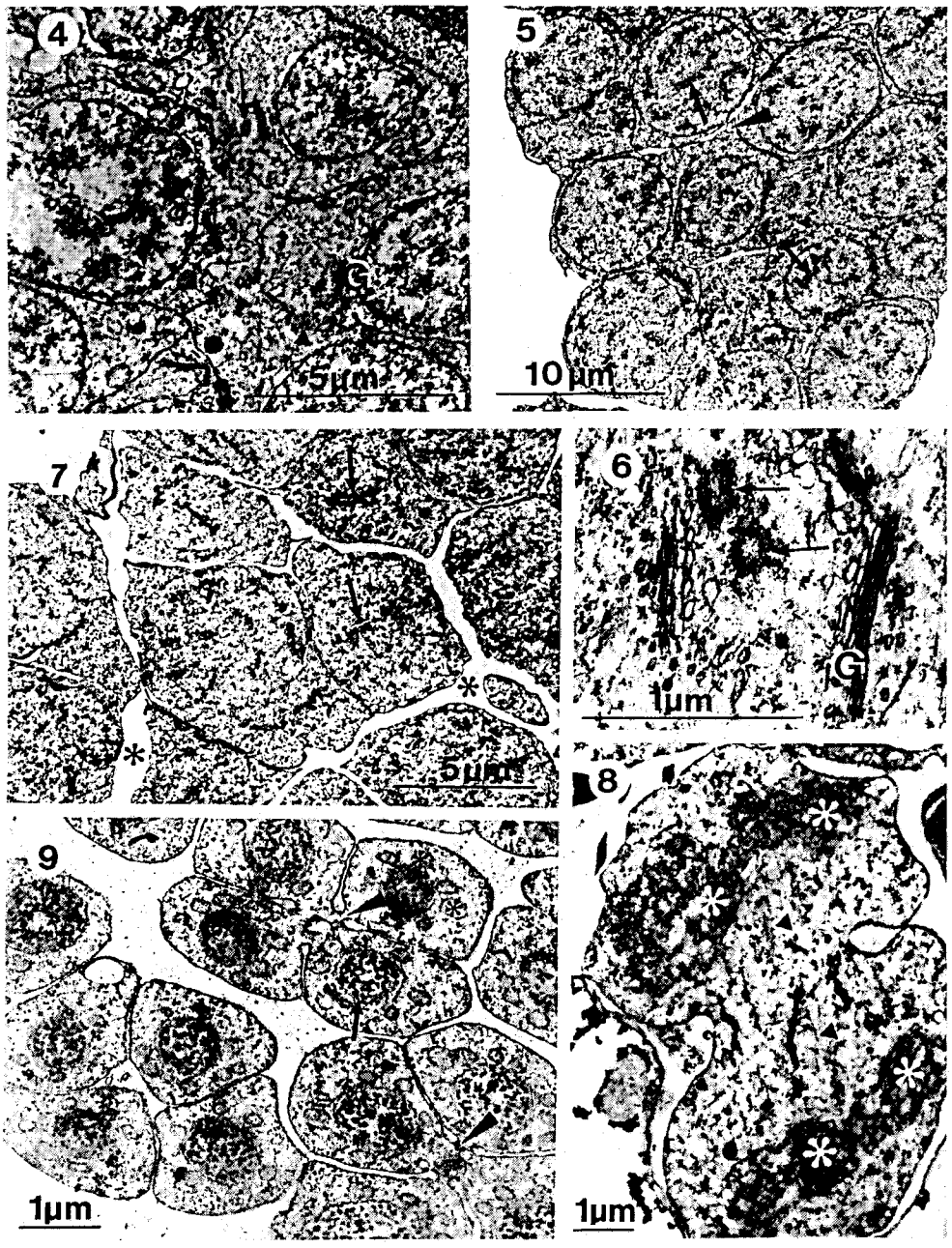
4
G
5µm
5
10µm
7
*
*
5µm
6
G
1µm
8
1µm
9
1µm

Spermiogenesis

Spermatids are also interconnected by cytoplasmic bridges (Fig. 9). However, this type of bridge shows considerable differences from the fusomes of earlier stages. The cell membrane in the tetrad bridges show neither accumulations of electron-dense material nor the characteristic electron-dense granules as observed in fusomes. Spermatid tetrads are not in cytoplasmic continuity with each other, because the fusomes between spermatogonia and spermatocytes break down at the end of stage 4. Tetrads float freely in the coelomic fluid. The four cells of a tetrad detach shortly before spermiogenesis is completed (stage 5). One of the first signs of spermiogenesis is the appearance of flocculent material within the spermatid nuclei (Fig. 9). This material is thought to represent chromatin in a certain state of condensation. Then flagellae emerge, and polarity is thus developed. The emerging flagellae mark the prospective posterior poles of the sperms (Fig. 10). The distal centriole is oriented perpendicular to the cell surface whereas the proximal centriole is typically oriented with its long axis perpendicular to the distal centriole and parallel to the long axis of the nucleus (Fig. 11). The spermatids of the tetrad now elongate parallel to each other with the cell bridges remaining intact (Fig. 12). The proacrosomal vesicles migrate to the anterior ends of the spermatids and fuse to form the acrosomes proper. Immediately beneath the acrosome a subacrosomal plate is formed, and the axial rod starts to penetrate the elongated nucleus (Fig. 13). At that time the spermatids have elongated considerably, and the process of nuclear condensation continues (Fig. 12). The tetrads are still in cytoplasmic continuity. The cell bridges are situated relatively close to the posterior poles of the spermatids. In some instances, the flagellae of the spermatids have been found to beat while still in the coelomic fluid. Finally the spermatids detach from each other, and nuclear condensation proceeds (Figs 14, 15). The condensation of nuclear material is characterized by the temporary appearance of globular, electron-dense nodules (Fig. 14). The number of these nodules seems to increase, which results in a denser packing of these granules (Fig. 15).

Sperm morphology

The head of a mature spermatozoon is approximately 10 μm in length and 1.5 μm in diameter (Figs 16, 17a, b, c). The volume of the nucleus is approximately 4 μm^3. The bell-

Fig. 4. Golgi stacks (G) and centrioles (arrow) are regularly found close to cell bridges (arrowheads) in spermatocytes

Fig. 5. EM of stage 2 cluster at transition to stage 3. Clusters tend to divide into smaller subclusters which are temporarily held together by pseudopodia-like processes (arrowhead). Synaptonemal figures (arrows) indicate the beginning of meiosis

Fig. 6. EM of Golgi stacks (G) and centrioles (arrows) in the immediate vicinity of cell bridges between primary spermatocytes

Fig. 7. EM of stage 3 primary spermatocytes. Asterisks mark relatively large intercellular clefts. Note the presence of synaptonemal figures (arrows)

Fig. 8. EM of first meiotic division in late stage 3 cells. Asterisks – chromosomes; arrowheads – spindle microtubules

Fig. 9. EM of spermatid tetrads (stage 4). Arrowheads indicate cell bridges that are different from cell bridges in primary spermatocytes. Mitochondria (asterisks) surround nuclei in which chromatin condensation has just started with the formation of electron-dense nodules (arrow)

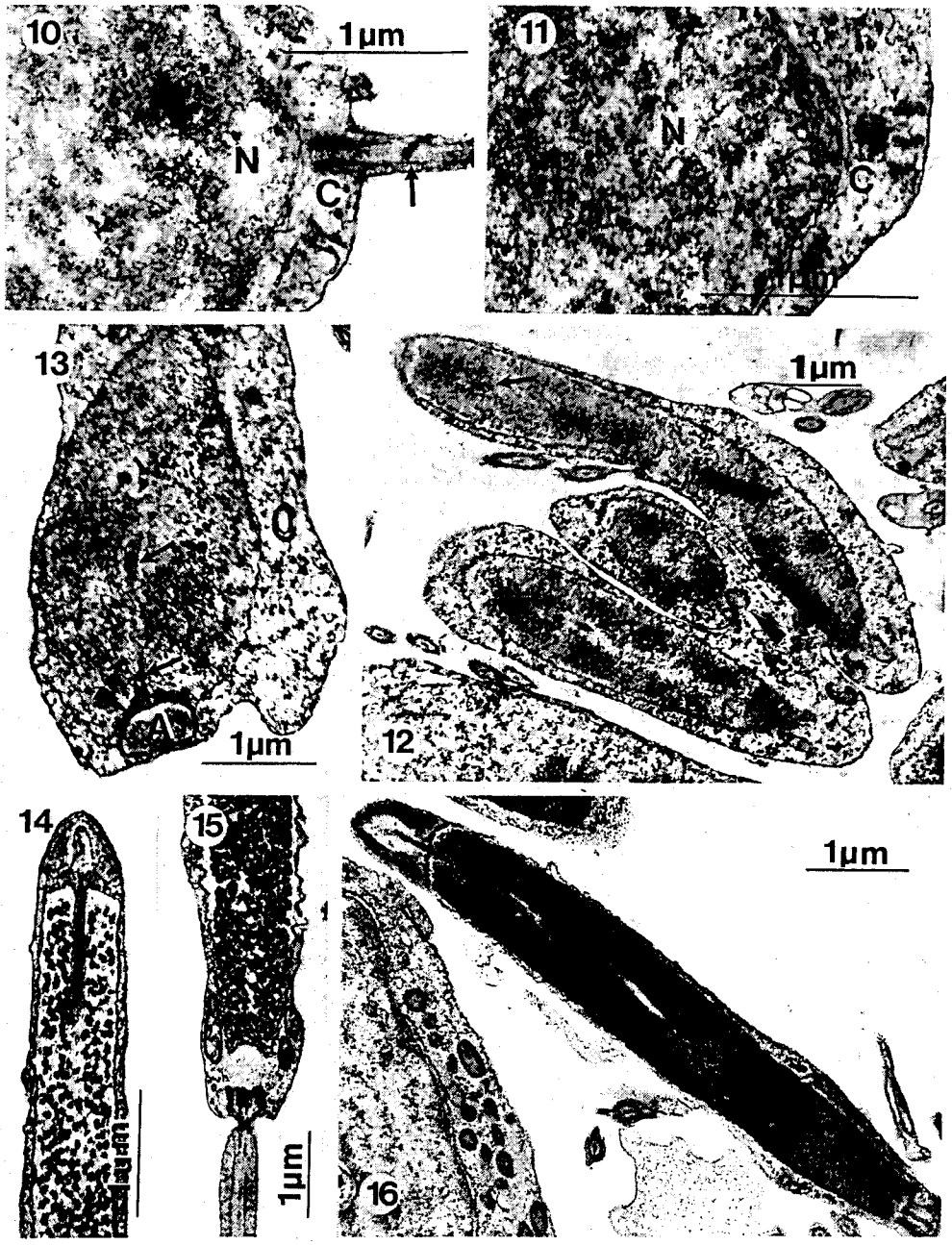
10
1µm
N
C
11
N
C
13
C
A
1µm
12
1µm
14
15
1µm
16
1µm

shaped acrosome takes about 20 % of the head length. It encloses a subacrosomal space. A subacrosomal plate separates the acrosome from the nucleus (Figs 16, 17a). The subacrosomal plate is penetrated by the axial rod which extends from the subacrosomal space into the nucleus (Figs 14, 16, 17b, c). There are no structural contacts between the rod and either the acrosome or the nucleus. The rod ends within the posteriorly closed nucleus and does not contact the basal body at the posterior end of the nucleus. The nucleus proper is long and slender, and the chromatin appears to be much more homogeneous than in the spermatid nucleus. The posterior end of the nucleus tapers somewhat. Long mitochondria surround the tapered part of the nucleus and the basal body of the tail thus forming an inconspicuous middle piece (Figs 15, 17a). As judged from their size and number, sperm mitochondria possibly have been formed by fusion of normal sized mitochondria during spermiogenesis. However, actual fusion of mitochondria has not been observed. Nine arms of the basal body connect the flagellum to the middle piece. It is thought that the paddle-wheel like structure of the basal body (Figs 17d, e) acts as an anchor for the flagellum. The microtubule doublets of the basal body directly extend into the flagellar axoneme. The proximal flagellar membrane forms two lateral folds (Fig. 17a, f) which may be interpreted as structures that enhance the thrust of the flagellum. The more distal parts of the flagellum do not display any membrane protrusions (Fig. 17a, g). The microtubule doublets of the basal body as well as those of the axoneme of the flagellum are arranged in the typical 9 + 2 pattern (Fig. 17d–g).

DISCUSSION

Spermatogenesis in *Platynereis massiliensis* does not differ dramatically from its sibling *Platynereis dumerilii* (Schiedges, 1981; Hofmann et al., 1986; Pfannenstiel et al., 1987). The processes of spermiogenesis are essentially the same in these two sibling species and in other nereid species (for review see Sawada, 1984). In *P. massiliensis* spermiogenesis leads to a long and slender sperm head whereas *P. dumerilii* sperm show a spherical nucleus. Thus sperm morphology is strikingly different in the two species, although it has been brought about by very similar cellular events.

The so-called primitive type of sperm with a more or less spherical head is thought to be typical of aquatic invertebrates with external fertilization. Obviously, sperm morphology reflects the respective mode of sperm transfer, since in a number of species with

---

Fig. 10. EM of posterior part of spermatid with emerging flagellum. The microtubules of the distal centriole (C) continue as axoneme microtubules (arrow) into the flagellum. N – nucleus

Fig. 11. EM of posterior end of spermatid. Centriole (C) forms the basal body of the flagellum close to the nucleus (N). Note that the centrioles are still perpendicular to each other

Fig. 12. EM of elongating spermatid tetrad. Nuclear condensation is in progress. Axial rods (arrows) form inside the nuclei. Spermatids are still in cytoplasmic continuity (arrowhead)

Fig. 13. EM of anterior end of spermatid. Axial rod (arrows) appears to be in close contact with a subacrosomal plate (arrowhead). Proacrosomal vesicles give rise to the acrosome (A)

Fig. 14. EM of anterior end of early spermatozoon. Axial rod penetrates the subacrosomal plate. Loosely packed electron-dense nodules represent an intermediate stage of nuclear condensation

Fig. 15. EM of posterior part of almost mature spermatozoon. Mitochondria surround the posterior region of nucleus; centrioles have formed the basal body of the flagellum. Electron-dense chromatin particles are densely packed

Fig. 16. EM of mature spermatozoon. Note tightly packed chromatin

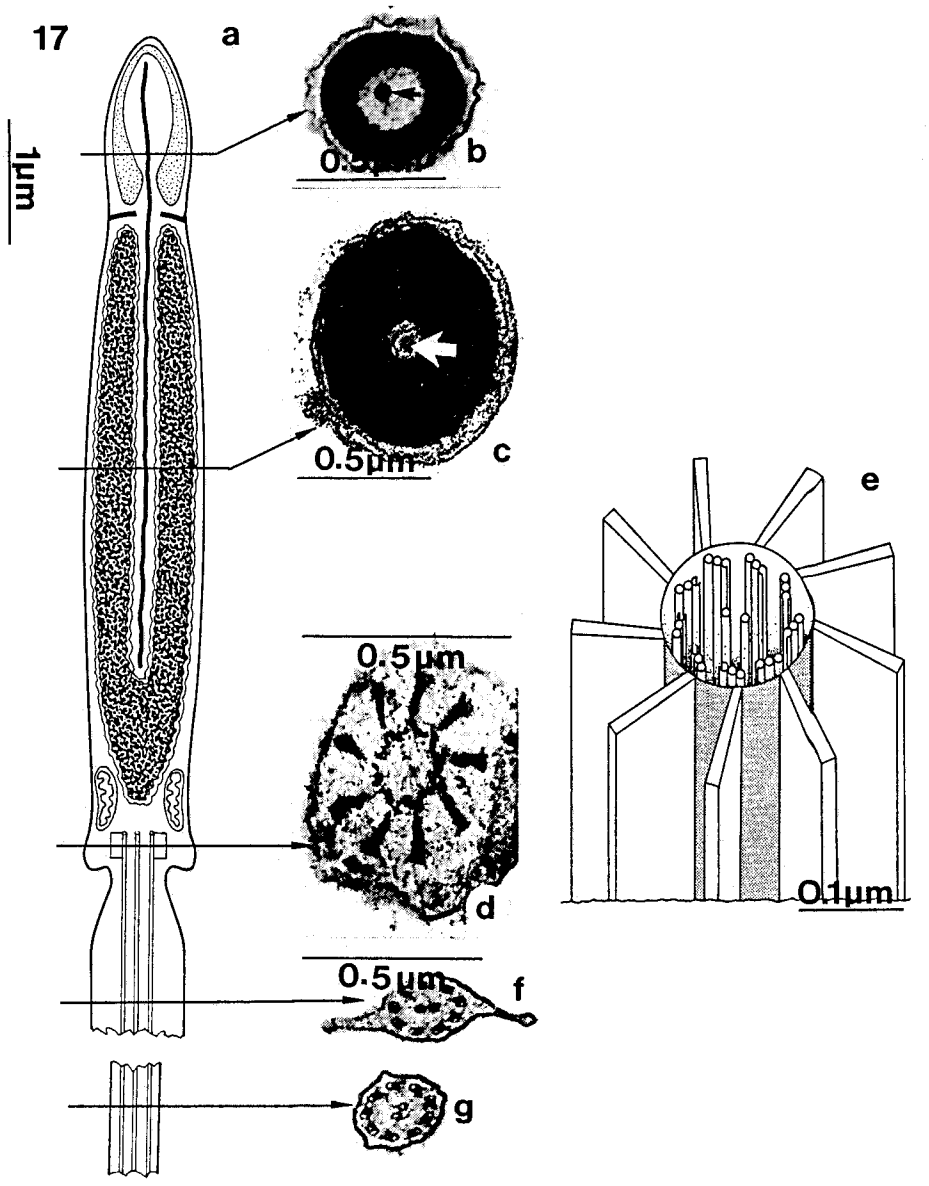

Fig. 17. Aspects of mature spermatozoon. a – schematic representation of spermatozoon; b – EM of acrosome in cross-section; note axial rod (arrow); c – EM of nucleus in cross section; note axial rod (arrow) and densely packed chromatin; d – EM of basal body in slightly oblique section; e – schematic representation of basal body; nine bars surround 9 + 2 structure forming a paddle-wheel structure; f – EM of proximal flagellum in cross-section; note lateral folds of flagellar membrane; g – EM of distal flagellum in cross section; note the absence of lateral folds

aberrant types of sperm transfer, sperm morphology is also altered. This can be true even for species within the same genus (Franzén, 1956, 1977; Sawada, 1984; Westheide, 1984). As has been pointed out in a preliminary study, sperm morphology in *P. dumerilii* is of the primitive type whereas *P. massiliensis* sperm are of an aberrant type (Pfannenstiel et al., 1987). Accordingly, *P. dumerilii* releases its gametes freely into the sea-water, while *P. massiliensis* pairs perform a pseudocopulation within a brooding tube. However, the fact that sperm morphology is of adaptive significance does not tell us anything about the actual requirements during sperm transfer and fertilization to which sperm morphology is adapted. In the dorvilleid *Ophryotrocha,* for example, the motile apparatus of sperm is almost completely reduced to a so-called flagellar equivalent (Troyer & Schwager, 1979; Pfannenstiel & Grünig, 1989). But despite the fact that in both *P. massiliensis* and *Ophryotrocha* sperm transfer is accomplished during pseudocopulation, sperm morphology is not at all the same. The differences in sperm morphology between the siblings *P. massiliensis* and *P. dumerilii* are striking. They mainly concern the sperm head. In *P. massiliensis* the sperm head is long and cylindrical as has been documented in the present study while the sperm head in *P. dumerilii* is spherical and much shorter. The volumes of the nuclei in both *P. massiliensis* (4 μm^3) and *P. dumerilii* (6 μm^3) appear to range in the same order of magnitude. At present, we cannot offer any evidence as to the nature of the selective pressure that has brought about different sperm in these nereid sibling species.

Acknowledgements. This work was supported by the Deutsche Forschungsgemeinschaft (Pfa 116/4). We would like to thank C. Grünig for excellent technical assistance, and D. K. Hofmann for his critical comments on the manuscript.

LITERATURE CITED

Franzén, Å., 1956. On spermiogenesis, morphology of the spermatozoon, and biology of fertilization among invertebrates. – Zool. Bidr. Uppsala *31,* 355–482.

Franzén, Å., 1977. Sperm structure with regard to fertilization biology and phylogenetics. – Verh. dt. zool. Ges. *1977,* 123–138.

Hauenschild, C., 1951. Nachweis der sogenannten atoken Geschlechtsform des Polychaeten *Platynereis dumerilii* Aud. et M.-Edw. als eigene Art auf Grund von Zuchtversuchen. – Zool. Jb. (Allg. Zool. Physiol. Tiere) *63,* 107–128.

Hauenschild, C., 1966. Der hormonale Einfluß des Gehirns auf die sexuelle Entwicklung bei dem Polychaeten *Platynereis dumerilii.* – Gen. Comp. Endocrinol. *6,* 26–73.

Hauenschild, C., 1970. Die Zucht von niederen marinen Wirbellosen und ihre Anwendung in der experimentellen Zoologie. – Helgoländer wiss. Meeresunters. *20,* 249–263.

Hofmann, D. K., Boes, J. & Hanske, M., 1986. Spermatogenesis in the polychaete *Platynereis dumerilii.* – In: Advances in invertebrate reproduction. Ed. by M. Porchet, J.-C. Andries & A. Dhainaut. Elsevier, Amsterdam, *4,* 1–520.

Pfannenstiel, H.-D. & Grünig, Ch., 1989. Spermatogenesis in the protandric polychaete *Ophryotrocha puerilis puerilis* (Dorvilleidae). In: Proceedings of the 2nd International Polychaete Conference. Ed. by J. B. Kirkegaard & M. E. Petersen. Brill, Leiden (in press).

Pfannenstiel, H.-D., Grünig, Ch. & Lücht, J., 1987. Gametogenesis and reproduction in nereidid sibling species *(Platynereis dumerilii* and *P. massiliensis).* – Bull. biol. Soc. Wash. *7,* 272–279.

Sawada, N., 1984. Electron microscopical studies of spermatogenesis in polychaetes. – Fortschr. Zool. *29,* 99–114.

Schiedges, I., 1981. Spermatogenese, Metamorphose, Regeneration und deren Beziehungen zum endokrinen System bei *Platynereis dumerilii.* – Diss. Univ. Köln, 94 pp.

Troyer, D. & Schwager, P., 1979. Ultrastructure and evolution of a sperm: Phylogenetic implications of altered motile machinery in *Ophryotrocha puerilis* spermatozoa. – Eur. J. Cell Biol. *20,* 174–176.

Westheide. W., 1984. The concept of reproduction in polychaetes with small body size: adaptations in interstitial species. – Fortschr. Zool. *29,* 265–287.